Two-photon laser spectroscopy of antiprotonic helium atoms, and the antiproton-to-electron mass ratio

2013 J. Phys.: Conf. Ser. 467 012006

(http://iopscience.iop.org/1742-6596/467/1/012006)

Journal of Physics: Conference Series **467** (2013) 012006 doi:10.1088/1742-6596/467/1/012006

Two-photon laser spectroscopy of antiprotonic helium atoms, and the antiproton-to-electron mass ratio

Masaki Hori

Max-Planck-Institut für Quantenoptik, Hans-Kopfermann-Strasse 1, 85748 Garching, Germany

E-mail: Masaki.Hori@mpq.mpg.de

Abstract. Some two-photon transitions in antiprotonic helium atoms at the deep UV wavelengths $\lambda = 139.8$–197.0 nm were recently studied by laser spectroscopy. The thermal Doppler broadening of the observed antiprotonic resonances were reduced by exciting the atoms with two counterpropagating laser beams of wavelengths $\lambda = 265$–417 nm. The resulting narrow spectral lines allowed the measurement of three transition frequencies in antiprotonic helium-3 and helium-4 isotopes with fractional precisions of 2.3–5 parts in 10^9. By comparing the results with three-body QED calculations, the antiproton-to-electron mass ratio was derived as 1836.1526736(23). We briefly review these experimental results that were presented in Ref. [1].

1. Introduction

Metastable antiprotonic helium ($\overline{p}\mathrm{He}^+$) is a three-body atom [1, 2, 3, 4] consisting of a helium nucleus, an electron in the 1s state, and an antiproton occupying a Rydberg state with high principal and angular momentum quantum numbers $n \sim \ell + 1 \sim 38$. The atom retains microsecond-scale lifetimes against antiproton annihilation in the helium nucleus, due to the fact that the antiproton orbital has a negligible overlap with the nucleus; the 1s electron protects the antiproton against collisions with other helium atoms. This longevity makes $\overline{p}\mathrm{He}^+$ especially amenable to precision laser spectroscopy [5, 6, 7]. The atomic transition frequencies of $\overline{p}\mathrm{He}^+$ have been calculated by three-body QED calculations to fractional precisions of 1×10^{-9} [8]. These calculations included relativistic and radiative recoil corrections up to order $m_e c^2 \alpha^6/h$, and nuclear size effects. By comparing the measured and calculated transition frequencies, the antiproton-to-electron mass ratio can be determined to parts-per-billion scale precision.

The ASACUSA collaboration at CERN [9] has measured some $\overline{p}\mathrm{He}^+$ transition frequencies in the optical region $0.3 - 1$ PHz with a fractional precision of $10^{-7} - 10^{-8}$, by single-photon laser spectroscopy [5, 6, 7]. The precision was limited by the Doppler broadening of the resonance lines which arose from the thermal motions of the $\overline{p}\mathrm{He}^+$ in the target. Unlike the atomic hydrogen case [10], it is difficult to cancel the first-order Doppler broadening by irradiating the atom with two equal-frequency photons and inducing a two-photon transition; the probabilities involved in these nonlinear transitions of the massive antiproton are too small (a few a.u.). In fact, calculations indicate that gigawatt-scale laser powers would be needed to excite the antiproton within the atom's microsecond-scale lifetime against annihilation [11].

In a recent experiment, two-photon transitions of the type $(n, \ell) = (n-2, \ell-2)$ [1] [Fig. 1(a)] were excited by utilizing the fact that the probability can be enhanced by factor $\sim 10^4$, to

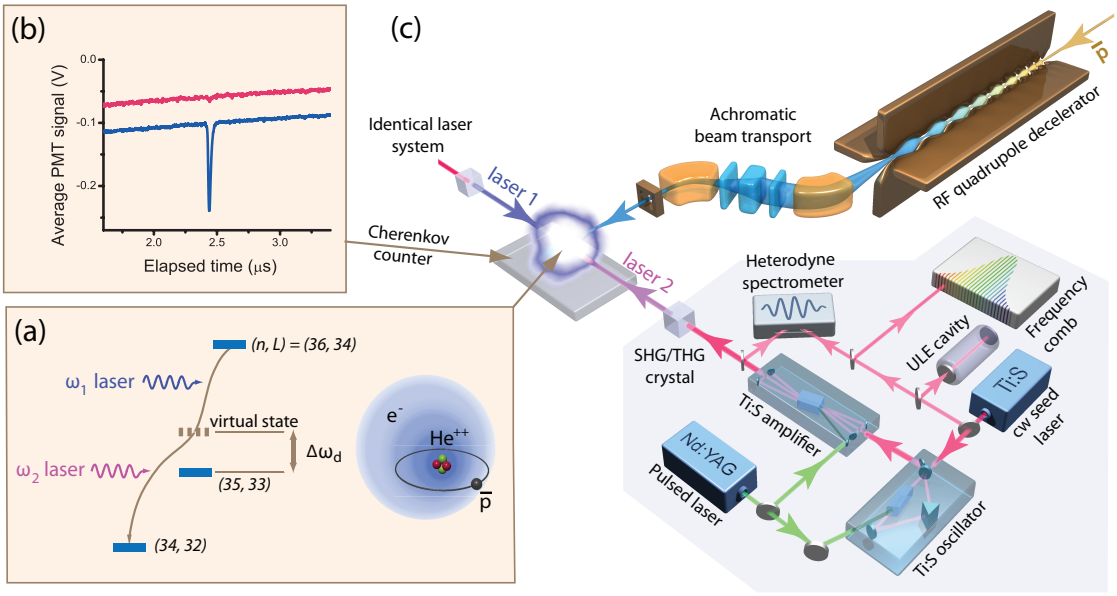

Figure 1. Schematic energy level diagram of $\overline{p}^4\mathrm{He}^+$ states involved in the two-photon transition $(n,\ell) = (36,34) \rightarrow (34,32)$ (a). The virtual intermediate state is tuned some $\Delta\omega_c \sim 10$ GHz from a real state $(35,33)$. Cherenkov detector signals for two-photon transition (b). Experimental layout (c). See Ref. [1] for details.

around $\sim 10^4$ a.u., if the counterpropagating beams have non-equal frequencies ν_1 and ν_2, such that the virtual intermediate state of the two-photon transition lies within a few GHz of a real $\overline{p}\mathrm{He}^+$ state $(n-1,\ell-1)$. The first-order Doppler width in the observed resonance lines can then be reduced by a factor $|\nu_1 - \nu_2|/(\nu_1 + \nu_2) \sim 1/20$.

2. Experiment

The two-photon transitions were induced between $\overline{p}\mathrm{He}^+$ states with microsecond and nanosecond-scale lifetimes against Auger emission of the electron. After Auger decay, the remaining two-body $\overline{p}\mathrm{He}^{2+}$ ion [12] was rapidly destroyed by Stark collisions with other helium atoms in the experimental target. The charged pions emerging from the resulting antiproton annihilations were detected by Cherenkov detectors [13] placed around the experimental target. The two-photon resonance condition between the counterpropagating laser beams and the $\overline{p}\mathrm{He}^+$ was thus revealed as a sharp spike in the rate of antiproton annihilations [Fig. 1(b)].

Megawatt-scale laser pulses of high spectral purity are needed to excite these nonlinear two-photon transitions, that have amplitudes of 10^3–10^4 a.u. We therefore developed two sets of Ti:Sapphire lasers [14] of pulse length 30-100 ns with a narrow spectral linewidth (~ 6 MHz). The laser system included continuous-wave (cw) lasers of wavelengths 728–940 nm, whose frequencies were measured to a precision of $< 1 \times 10^{-10}$ against a femtosecond optical frequency comb [15]. This beam was then used to seed a ring Ti:Sapphire oscillator and multipass amplifier which generated laser pulses of energy 50–100 mJ.

Nanosecond-scale changes in the refractive index of the Ti:Sapphire crystals during the amplification, as well as the so-called "mode-pulling" effects in the pulsed laser cavity [14], caused the laser linewidth to broaden and the frequency to shift by several tens MHz. This frequency chirp was measured using a heterodyne spectrometer, and corrected by intracavity electro-optic modulators located inside the Ti:Sapphire cavity. The spectral precision ($< 1.4 \times 10^{-9}$) of the

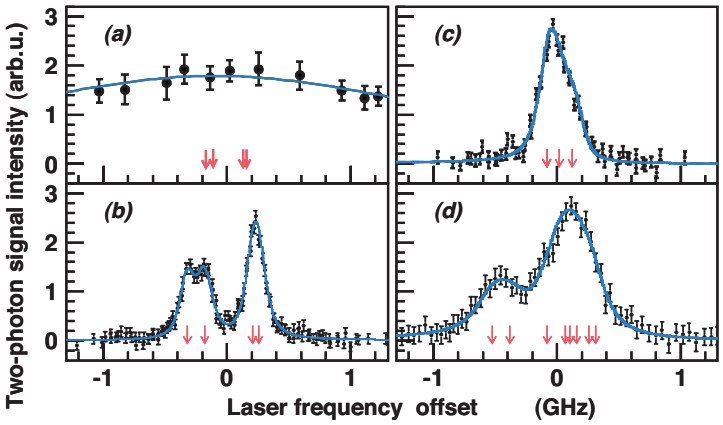

Figure 2. Doppler- and power-broadened profile of the single-photon resonance $(36, 34) \rightarrow (35, 33)$ of $\overline{p}^4\mathrm{He}^+$ (a). Sub-Doppler two-photon profiles of $(36, 34) \rightarrow (34, 32)$ (b) and $(33, 32) \rightarrow (31, 30)$ (c) of $\overline{p}^4\mathrm{He}^+$, and $(35, 33) \rightarrow (33, 31)$ of $\overline{p}^3\mathrm{He}^+$ (d). Solid lines indicate best fit of theoretical line profiles (see text) and partly overlapping arrows the positions of the hyperfine lines. From Ref. [1].

pulsed laser was verified by measuring some two-photon transition frequencies in Rb and Cs at wavelengths of 778 and 822 nm.

The Antiproton Decelerator (AD) facility of CERN provided 200-ns-long pulsed beams, which contained $\sim 10^7$ antiprotons of kinetic energy 5.3 MeV, at a repetition rate of 0.01 Hz [Fig. 1 (c)]. The antiprotons were decelerated to ~ 70 keV, by allowing them to pass through a 3-m-long radiofrequency quadrupole decelerator [6]. Secondary electron emission detectors measured the spatial profiles of the beam [16]. The antiprotons were allowed to stop in a cryogenic target chamber filled with ^{4}He or ^{3}He gas at temperature $T \sim 15$ K and pressure $p = 0.8 - 3$ mbar. Two, horizontally-polarized laser beams of energy density ~ 1 mJ/cm^2 fired through the target in a perpendicular direction to the antiproton beam excited the two-photon transitions.

The Cherenkov signal corresponding to some 10^7 $\overline{p}\mathrm{He}^+$ atoms is shown in Fig. 1(b), as a function of time elapsed since the arrival of antiproton pulses at the experimental target. Lasers of wavelengths $c/\nu_1 = 417$ and $c/\nu_2 = 372$ nm were tuned to the two-photon transition $(n, \ell) = (36, 34) \rightarrow (34, 32)$, so that the virtual intermediate state lay $\Delta\nu_d \sim 6$ GHz away from the real state $(35, 33)$. The annihilation spike which corresponds to the two-photon transition can be seen at $t = 2.4\mu$s. The intensity of the spike reflects the number of antiprotons populating state $(36, 34)$ [17, 18, 19]. When the 417-nm laser was tuned some ~ 0.5 GHz off the two-photon resonance condition, the signal disappeared as indicated in the same figure.

Fig. 2(b) shows the resonance profile which was measured by detuning the ν_1 laser to $\Delta\nu_d = -6$ GHz, whereas the ν_2 laser was scanned between -1 and 1 GHz around the two-photon resonance defined by $\nu_1 + \nu_2$. The linewidth (~ 200 MHz) of this two-photon resonance is more than an order of magnitude smaller than the Doppler- and power-broadened profile of the single-photon one $(36, 34) \rightarrow (35, 33)$ [Fig. 2(a)]. The two-peak structure, with a frequency interval of 500 MHz, arises due to the interaction between the electron spin and the orbital angular momentum of the antiproton. We also detected the $(33, 32) \rightarrow (31, 30)$ resonance of $\overline{p}^4\mathrm{He}^+$ at a wavelength of 139.8 nm, using lasers of $c/\nu_1 = 296$ nm and $c/\nu_2 = 265$ nm [Fig. 2(c)] detuned $\Delta\nu_d \sim 3$ GHz from state $(32, 31)$. All four hyperfine lines are much closer together (± 100 MHz). We also measured the $\overline{p}^3\mathrm{He}^+$ resonance $(35, 33) \rightarrow (33, 31)$ of $\lambda = 193.0$ nm [Fig. 2(d)] using lasers of 410 and 364 nm. This resonance profile contains eight partially-overlapping hyperfine

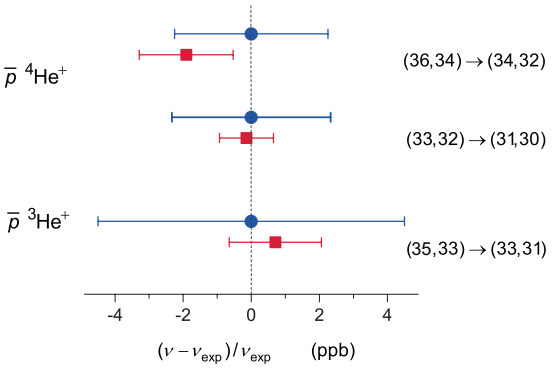

Figure 3. Fractional deviation between theoretical (squares) and experimental (circles) transition frequencies of $\bar{p}\mathrm{He}^+$ isotopes measured by two-photon laser spectroscopy. From Ref. [1].

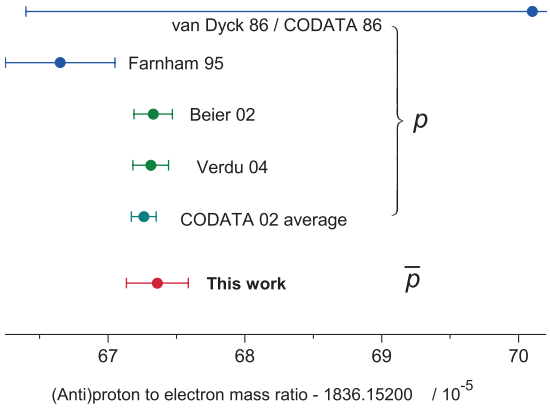

Figure 4. Antiproton-to-electron mass ratio determined in this work, compared with the proton-to-electron mass ratios measured in Penning trap experiments [22, 23, 24, 25] and the CODATA 2002 recommended value obtained by averaging them. From Ref. [1].

lines, which arose from the spin-spin interactions of the three constituent particles.

The spin-independent transition frequencies ν_{exp} were obtained by fitting these measured profiles with a theoretical lineshape (solid lines in Fig. 2) which was determined by numerically solving the rate equations of the two-photon process [11]. This included the transition rates, power and Doppler broadening effects, frequency modulation in the laser pulse, the experimentally-measured spatial and temporal profiles of the laser beam, and ac Stark effects. The positions of the hyperfine lines were fixed to the theoretical values calculated by Korobov [20], which have a precision of < 0.5 MHz. For the transition $(36, 34) \rightarrow (34, 32)$ in $\bar{p}^4\mathrm{He}^+$, the statistical uncertainty due to the finite number of atoms in the laser beam was estimated as 3 MHz. For the target densities studied here $\rho = (1-3)\times 10^{18}$ cm^{-3}, no significant collisional shift was observable within the experimental error. This agrees with quantum chemistry calculations [21], for which the predictions of 0.1–1-MHz collisional shifts in the single-photon lines agreed with experimental results [7] with a precision of $\leq 20\%$. Theoretical calculations [11] also show that magnetic Zeeman shifts are also small < 0.5 MHz. The ac Stark shift [11] was reduced to ≤ 5 MHz by adjusting the relative intensities of the two laser beams. Remaining ac Stark shifts were canceled to a level of 0.5MHz by systematically comparing the resonance profiles measured at positive and negative detunings $\pm\Delta\nu_d$ of the virtual intermediate state. The experimental uncertainty σ_{exp} was obtained as the quadratic sum of all these errors.

3. Results and conclusions

The experimental transition frequencies ν_{exp} (filled circles with error bars in Fig. 3) agree with the QED calculated ν_{th} values (squares) within a fractional precision of $(2-5)\times 10^{-9}$. The calculation uses the fundamental constants compiled in CODATA2002 [22], such as the ^{3}He- and ^{4}He-to-electron mass ratios, the Bohr radius, and Rydberg constant. The charge radii of the ^{3}He and ^{4}He nuclei give relatively small corrections to ν_{th} of $4-7$ MHz, whereas the correction from the antiproton radius is less than 1 MHz. The small contributions are due to the fact that the wavefunctions of the antiprotonic states with large ℓ-value have only a negligible

overlap with the helium nucleus. The theoretical precision of $\nu_{\rm th}$ is now mainly limited by the uncalculated radiative corrections of order $m_e c^2\alpha^8/h$ [8], but higher-order corrections are now being calculated. When the antiproton-to-electron mass ratio $M_{\overline{p}}/m_e$ in these calculations was increased by a relative amount of 10^{-9}, the $\nu_{\rm th}$-value changed by 2.3–2.8 MHz. By minimizing the difference between $\nu_{\rm th}$ and $\nu_{\rm exp}$ and considering the systematic errors, we obtained the antiproton-to-electron mass ratio as,

$$M_{\overline{p}}/m_e = 1836.1526736(23), \tag{1}$$

which yielded the best agreement between theoretical and experimental frequencies. The uncertainty includes the statistical and systematic experimental, and theoretical contributions of 18×10^{-7}, 12×10^{-7}, and 10×10^{-7}. This is in good agreement with previous measurements[22, 23, 24, 25] of the proton-to-electron mass ratio (Fig. 4), which have a similar experimental precision. By assuming that CPT invariance is valid (i.e, $M_{\overline{p}} = M_p = 1.00727646677(10)$ u), we further derived a value for the electron mass, $m_e = 0.0005485799091(7)$ u, from this experimental result on $\overline{p}{\rm He}^+$ [1].

Hughes and Deutch [26, 27] has constrained any difference between the antiproton and proton charges and masses $\delta_Q = (Q_p + Q_{\overline{p}})/Q_p$ and $\delta_M = (M_p - M_{\overline{p}})/M_p$ to better than 2×10^{-5}. To do this, they combined X-ray spectroscopic data of antiprotonic atoms (proportional to $Q_{\overline{p}}^2 M_{\overline{p}}$) and the cyclotron frequency ($\propto Q_{\overline{p}}/M_{\overline{p}}$) of antiprotons confined in magnetic Penning traps measured to a higher precision. We improved this limit by studying the linear dependence of δ_M and δ_Q on $\nu_{\rm th}$ of $\overline{p}{\rm He}^+$, i.e., $\delta_M\kappa_M + \delta_Q\kappa_Q < |\nu_{\rm exp} - \nu_{\rm th}|/\nu_{\rm exp}$ [2]. For the three $\overline{p}{\rm He}^+$ transitions studied in this work, the constants were estimated as $\kappa_M = 2.3 - 2.8$ and $\kappa_Q = 2.7 - 3.4$, whereas the right side of this equation was evaluated by averaging over the three transitions as $< (8 \pm 15)\times10^{-10}$. Meanwhile the constraint of $(Q_{\overline{p}}/M_{\overline{p}})/(Q_p/M_p) + 1 = 1.6(9)\times10^{-10}$ from the TRAP experiment [28, 29] implies that $\delta_Q \sim \delta_M$. We conclude from this that any deviation between the charges and masses of protons and antiprotons are less than 7×10^{-10} at 90% confidence level [1].

We are currently attempting to further improve the experimental and theoretical uncertainties in these experiments, by e.g., cooling the atoms to lower temperature and improving the quality of the antiproton beam.

Table 1. Spin-averaged transition frequencies of $\overline{p}{\rm He}^+$. Experimental values show respective total, statistical and systematic errors in parentheses. Theoretical values (From Ref. [8] and V. I. Korobov, private communication) show respective uncertainties from uncalculated QED terms and numerical errors in parentheses. From Ref. [1].

Isotope	Transition $(n,\ell) \to (n-2,\ell-2)$	Transition frequency (MHz) Experiment	Theory
$\overline{p}^4{\rm He}^+$	$(36,34) \to (34,32)$	1,522,107,062(4)(3)(2)	1,522,107,058.9(2.1)(0.3)
	$(33,32) \to (31,30)$	2,145,054,858(5)(5)(2)	2,145,054,857.9(1.6)(0.3)
$\overline{p}^3{\rm He}^+$	$(35,33) \to (33,31)$	1,553,643,100(7)(7)(3)	1,553,643,100.7(2.2)(0.2)

Acknowledgments
This work was supported by the European Research Council (ERC-Stg), Monbukagakusho (grant no 20002003), Hungarian Research Foundation (K72172), and the Austrian Federal Ministry of

Science and Research. I thank the ASACUSA collaborators, CERN AD and PS operational staff, the CERN cryogenics laboratory, J. Alnis, D. Bakalov, J. Eades, R. Holzwarth, V.I. Korobov, M. Mitani, W. Pirkl, and T. Udem.

References

[1] Hori M *et al.* 2011 *Nature* **475** 484
[2] Hayano R S, Hori M, Horváth D and Widmann E 2007 *Rep. Prog. Phys.* **70** 1995
[3] Condo G T 1964 *Phys. Lett.* **9** 65
[4] Russel J E 1969 *Phys. Rev. Lett.* **23** 63
[5] Hori M *et al.* 2001 *Phys. Rev. Lett.* **87** 093401
[6] Hori M *et al.* 2003 *Phys. Rev. Lett.* **91** 123401
[7] Hori M *et al.* 2006 *Phys. Rev. Lett.* **96** 243401
[8] Korobov V I 2008 *Phys. Rev. A* **77** 042506
[9] Hori M and Walz J 2013 *Progress in Particle and Nuclear Physics* doi:10.1016/j.ppnp.2013.02.004
[10] Parthey Ch G *et al.* 2011 *Phys. Rev. Lett.* **107** 203001
[11] Hori M and Korobov V I 2010 *Phys. Rev. A* **81** 062508
[12] Hori M *et al.* 2005 *Phys. Rev. Lett.* **94** 063401
[13] Hori M *et al.* 2003 *Nucl. Instrum. Methods Phys. Res. A* **496** 102
[14] Hori M and Dax A 2009 *Opt. Lett.* **34** 1273
[15] Udem Th, Holzwarth R and Hänsch T W 2002 *Nature* **416** 233
[16] Hori M 2005 *Rev. Sci. Instrum.* **76** 113303
[17] Hori M *et al.* 2002 *Phys. Rev. Lett.* **89** 093401
[18] Hori M *et al.* 2004 *Phys. Rev. A* **70** 012504
[19] Hori M *et al.* 1998 *Phys. Rev. A* **57** 1698; 1998 *Phys. Rev. A* **58** 1612
[20] Korobov V I 2006 *Phys. Rev. A* **73** 022509
[21] Bakalov D *et al.* 2000 *Phys. Rev. Lett.* **84** 235
[22] Mohr P J, Taylor B N and Newell D B 2008 *Rev. Mod. Phys.* **80** 633
[23] Farnham D L, Van Dyck Jr. R S, Schwinberg P B 1995 *Phys. Rev. Lett.* **75** 3598
[24] Beier T *et al.* 2002 *Phys. Rev. Lett.* **88** 011603
[25] Verdú J *et al.* 2004 *Phys. Rev. Lett.* **92** 093002
[26] Hughes R J and Deutch B I 1992 *Phys. Rev. Lett.* **69** 578
[27] Nakamura K *et al.* 2010 *J. Phys.* **G37** 075021
[28] Gabrielse G *et al.* 1999 *Phys. Rev. Lett.* **82** 3198
[29] Thompson J K, Rainville S and Pritchard D E 2004 *Nature* **430** 58